Polymer 54 (2013) 5525–5533

Contents lists available at ScienceDirect

Polymer

journal homepage: www.elsevier.com/locate/polymer

Preparation of near-infrared absorbing composites comprised of conjugated macroligands on the surface of PbS nanoparticles

Jinming Zhang [a], Lydia Bahrig [b], Andreas Puetz [c], Ioannis Kanelidis [a], Daniel Lenkeit [a], Simon Pelz [a,1], Stephen G. Hickey [b], Michael F.G. Klein [c], Alexander Colsmann [c], Uli Lemmer [c], Alexander Eychmüller [b], Elisabeth Holder [a,*]

[a] Functional Polymers Group and Institute of Polymer Technology, University of Wuppertal, Gaußstr. 20, D-42097 Wuppertal, Germany
[b] Physical Chemistry and Electrochemistry, Technische Universität Dresden, Bergstr. 66b, D-01062 Dresden, Germany
[c] Light Technology Institute, Karlsruhe Institute of Technology (KIT), Engesserstr. 13, D-76131 Karlsruhe, Germany

ARTICLE INFO

Article history:
Received 25 May 2013
Received in revised form
15 August 2013
Accepted 16 August 2013
Available online 24 August 2013

Keywords:
Conjugated polymers
PbS nanocrystals
Functionalization

ABSTRACT

We report a facile macroligand strategy towards the synthesis of low-bandgap inorganic-organic composites comprised of semiconductor PbS nanoparticles and functional copolymers. For this, thiol-functional thiophene-based macroligands have been used as coligands for PbS nanoparticles. Thus, solution processable organic-inorganic hybrid materials with absorption in the near-infrared have been obtained. The resulting nanoparticle-polymer composites were characterized in detail by optical and FT-IR spectroscopy as well as TEM showing their potential as novel functional inorganic-organic hybrid materials when applied in initial proof-of-concept hybrid photovoltaic devices.

1. Introduction

Recent reviews reported that conjugated polymer-nanocrystal hybrid systems [1–9] could become a low cost material for photovoltaic cells, light emitting diodes, photodetectors and other devices in the future [10,11]. Moreover, it was shown that the ligand exchange on the PbS nanoparticles (NPs) revealed positive effects on the photovoltaic performance of such systems [12,13]. Thiophene-based conjugated alternating copolymers are in the focus due to their anticipated performance in many applications as mentioned above, paired with their rather undemanding synthetic availability using palladium-catalyzed cross-coupling reactions like Stille [14] or Suzuki [9] reactions. Other procedures of use are Grignard metathesis (GRIM) [15] or Yamamoto [9] reactions, which are mostly used for the preparation of homopolymers. GRIM is often used for the preparation of high quality regio-regular polymers like regio-regular poly(3-hexylthiophene-2,5-diyl) (rrP3HT) [9,15]. Since about a decade, functional thiophene-based molecules are, amongst other polymers, used for the preparation of various hybrid materials [9,16,17]. First results using low-bandgap copolymers in hybrid systems have lately been introduced [18]. Interestingly, the optical properties [19] of semiconductor NPs are determined by the quantum confinement effect [20]; their emission color and electronic levels can be finely tuned within a single synthetic route, not only by choice of NP material, but also by choice of NP size. A typical semiconductor NP, which can also be thought of as a colloidal quantum dot, consists of an inorganic core, comparable or smaller in size than the Bohr exciton diameter of the corresponding bulk material, surrounded ("passivated") by an organic shell of ligands. Bulk PbS [21,22] and PbSe [23] materials have a cubic (rock salt) crystal structure, a narrow direct bandgap (0.28–0.41 eV at 300 K) and an extraordinary large exciton Bohr radius (18 nm for PbS and 46 nm for PbSe respectively, the latter is about eight times larger than that of CdSe) [24–28]. Note, only few materials like InAs exist, having similar large Bohr radii like PbSe particles [28]. As particle volume to Bohr radii ratios of 0.04 can be obtained, size quantization effects are much more pronounced and the simple electronic and vibrational spectra of the nanoparticles allow their application in IR laser technologies, IR detectors, long-wavelength imaging, solar energy panels, bio-assays in water and window coatings [25]. PbS nanoparticles have been synthesized in diverse media like glasses [29,30], polymer matrices [31–33],

* Corresponding author. Tel.: +49 202 439 3879; fax: +49 202 439 3880.
E-mail addresses: andreas.puetz@kit.edu (A. Puetz), holder@uni-wuppertal.de (E. Holder).
[1] Present address: Institute of Physical Chemistry, University of Cologne, Germany.

0032-3861/$ – see front matter © 2013 Elsevier Ltd. All rights reserved.
http://dx.doi.org/10.1016/j.polymer.2013.08.038

aqueous solutions [34–36] or liquid crystals [37], using a variety of methods such as hot injection [38] sonochemical [39,40] or electrochemical techniques [41,42]. To date, high quality lead sulfide nanoparticles with respect to size distribution and optical emission have been attained by hot injection procedures using oleic acid and tri-*n*-octylphosphine as capping ligands and carrying out the reaction in different solvent mixtures of octadecene, tri-*n*-octylphosphine and oleic acid at an injection temperature of 150 °C. The nanoparticle's average size could be reduced when reducing the injection temperature of *bis*(trimethylsilyl)sulfide or the amount of oleic acid, spanning the absorption spectra due to their tunable sizes from 800 to 1800 nm.

In our approach, four alternating copolymers were synthesized by means of Stille-couplings, targeting donor–donor and donor-acceptors-donor structures. For the donor–donor structures, two copolymers were fabricated, based on thiophene and 3-hexylthiophene as building blocks where the synthesized copolymer was endcapped with the functional endcapper 4-bromobenzenethiol. The two donor-acceptor-donor copolymers were built from thiophene and 4,7-*bis*-(3-hexyl-thiophen-2-yl)-benzo-[*c*][1,2,5]-thiadiazole being furthermore endcapped with 4-bromobenzenethiol introducing a surface-active thiol-function to the copolymer [43]. All copolymers were fully characterized and revealed bandgaps in-between 1.80-1.85 eV in thin films. Due to their thiol-end groups, the copolymers may function to attach to a variety of nanoparticles and were therefore treated with PbS nanoparticles in a ligand exchange procedure, resulting in two novel PbS-based nanocomposites with prospects for use in hybrid photovoltaic devices.

2. Experimental part

2.1. Instrumentation

The microwave-supported organic syntheses was carried out with a CEM discover microwave with an electrical power of 300 W. Polymerization took place under temperature and compression-control. Details are described in Ref. [44].

^{1}H and ^{13}C nuclear magnetic resonance (NMR) spectra were recorded in deuterated chloroform ($CDCl_3$) with tetramethylsilane (TMS) as internal standard on a Bruker ARX 400 nuclear magnetic resonance spectrometer. The chemical shift δ is given in ppm. Mass spectra were obtained using a Bruker micrOTOF instrument equipped with an electrospray ionization source (ESI-MS) and on a Biflex II matrix-assisted laser desorption/ionization time-of-flight mass spectrometry (MALDI-TOFMS) system (Bruker Daltonics GmbH). For the sample preparation, 1 mg/mL of the polymer, 10 mg/mL dithranol and 0.1 mg/mL AgTFA were solubilized as mixture in THF in a ratio of 1:10:0.1. This mixture was transferred to the sample holder (2 μL) and subsequently analyzed in the refection mode detecting positive ions. Gel permeation chromatography (GPC) analysis was carried out on a Jasco AS950 apparatus using Jasco UV-2070, Jasco RI-930 and Viscotek T60 as detectors (column MZSD of particle size 5 μm, eluent chloroform). For the determination of the molecular weights, a calibration based on polystyrene standards was applied. The elemental analysis data were obtained by using a Vario Elemental EL analyzer. Infrared studies were conducted on a JASCO FT/IR-4200 Fourier-transform infrared spectrometer. Ultraviolet-visible measurements (UV-vis) were performed on a Jasco V-550 spectrophotometer (1 cm cuvette, chloroform) at concentrations of 3.3×10^{-6} mol/L for the copolymers. Fluorescence spectroscopic measurements were done on a Cary Eclipse fluorescence spectrophotometer (1 cm cuvette, chloroform) at concentrations of 3.3×10^{-6} mol/L for the copolymers. The film measurements were performed by using a concentration of 1 mg/mL copolymer in chloroform for the preparation of the respective films. Transmission electron microscopy (TEM) has been performed using a Tecnai T20 microscope operating at 200 kV (FEI). The sample preparation followed the procedure used in ref. 1. The optical characterization of the nanoparticles and composites were performed on a Cary 5000 Varian absorption spectrometer. Measurements in the UV-regime were conducted on a Cary 50 Varian absorption spectrometer. FT-IR spectra were measured on a Nicolet 8700 spectrometer from Thermo Scientific.

2.2. Materials

All reactions were carried out under inert conditions (argon). *N*-Bromosuccinimide was purchased from ABCR, thiophene from Acros, 2-(3-hexylthiophen-2-yl)-4,4,5,5-tetramethyl-1,3,2-dioxaborolane, 4-bromobenzenethiol, 2,1,3-benzothiadiazole, 3-hexylthiophene and trimethyltin chloride 1 M in *n*-hexane from Aldrich. 2,5-Dibromo-3-hexylthiophene (**M1**) [47], 2,5-*bis*-(trimethylstannyl)thiophene (**M2**) [48], 4,7-dibromo-2,1,3-benzothiadiazole (**1**) [52], 4,7-*bis*-(3-hexyl thiophen-2-yl)benzo[*c*][1,2,5]thiadiazole (**2**) [53] and 4,7-*bis*-(5-bro-mo-3-hexylthiophen-2-yl)benzo[*c*][1,2,5]thiadiazole (**M3**) [54] were synthesized according to literature procedures. All polymerizations were performed in extra dry THF (Acros) according to literature known procedures [44].

For the preparation of the PbS nanoparticles and their nanocomposites, THF, *N*,*N*-dimethylformamide, oleic acid, thioacetamide and lead acetate trihydrate were purchased from Aldrich, diphenylether and ethanol from Acros, tri-*n*-octylphosphine from Fluka and *n*-butanol from AppliChem.

2.3. Synthesis of the monomers

2.3.1. 2,5-Dibromo-3-hexyl-thiophene (*M1*) [47]

Colorless oil was obtained (6.78 g, 69%). ^{1}H NMR (400 MHz, $CDCl_3$): δ (ppm): 6.77 (s, 1H), 2.50 (t, 2H), 1.53 (m, 2H), 1.30 (t, 6H), 0.89 (t, 2H). ^{13}C NMR (400 MHz, $CDCl_3$): δ (ppm): 142.75, 130.70, 110.05, 107.68, 31.34, 29.32, 29.24, 28.56, 22.35, 13.86. ESI-MS m/z Calcd. For $C_{10}H_{14}Br_2S$ 326.09; Found 326.

2.3.2. 2,5-Bis-(trimethylstannyl)-thiophene (*M2*) [48]

A white solid (4.25 g, 46%) was obtained. ^{1}H NMR (400 MHz, $CDCl_3$): δ (ppm): 0.40 (s, 18 H, CH_2), 7.40 (s, 2 H, CH). ^{13}C NMR (400 MHz, $CDCl_3$): δ (ppm): 142.7, 135.5, −8.5. ESI-MS m/z Calcd. For $C_{10}H_{20}SSn_2$ 409.7; Found 410.

2.3.3. 4,7-Dibromo-2,1,3-benzothiadiazole (*1*) [52]

A yellowish solid was obtained (19.4 g, 90%). ^{1}H NMR (400 MHz, DMSO): δ (ppm): 7.94 (s, 2 H, CH). ^{13}C NMR (400 MHz, $CDCl_3$): δ (ppm): 152.8, 132.2, 113.8. ESI-MS m/z Calcd. For $C_6H_2Br_2N_2S$ $(M + H)^+$ 294; Found 294.

2.3.4. 4,7-Bis-(3-hexyl-thiophen-2-yl)-benzo[c][1,2,5]-thiadiazole (*2*) [53]

A yellow-orange oil was obtained (0.75 g, 70%). ^{1}H NMR (400 MHz, $CDCl_3$): δ (ppm): 7.65 (s, 2H), 7.43 (d, 2H), 7.10 (d, 2H), 2.66 (t, 4H), 1.61 (m, 2H), 1.20 (m, 12H), 0.81 (t, 6H). ^{13}C NMR (400 MHz, $CDCl_3$): δ (ppm): 154.53, 141.94, 132.42, 130.13, 129.45, 127.73, 126.07, 31.78, 30.88, 29.58, 29.32, 22.74, 14.23. ESI-MS m/z Calcd. For $C_{14}H_{10}Br_2$ 468.7; Found 468.

2.3.5. 4,7-Bis-(5-bromo-3-hexyl-thiophen-2-yl)-benzo[c][1,2,5]-thiadiazole (*M3*) [54]

A orange oil was obtained (0.82 g, yield 65%). ^{1}H NMR (400 MHz, $CDCl_3$): δ (ppm): 7.60 (s, 2H), 7.05 (s, 2H), 2.61 (m, 4H), 1.57 (m, 4H), 1.22 (m, 12H), 0.81 (t, 6H). ^{13}C NMR (400 MHz, $CDCl_3$): δ (ppm):

154.23, 142.75, 133.86, 132.30, 130.0, 126.94, 113.50, 31.81, 30.78, 29.71, 29.31, 22.79, 14.30. ESI-MS m/z Calcd. For $C_{26}H_{31}AgBr_2N_2S_3$ 733; Found $(M + H)^+$ 734.

2.4. Synthesis of the copolymers

2.4.1. Copolymers *P1* and *P2*—general procedure

2,5-Dibromo-3-hexyl-thiophene, 2,5-*bis*-(trimethylstannyl)-thiophene and $Pd(PPh_3)_4$ (5 mol%) were added together in a microwave tube. Under inert conditions, THF (4 mL) was added to the reaction system and was allowed to stir in the microwave for 12 min at 150 °C. After cooling down to room temperature, the reaction solution was poured in chloroform and the combined organic layers were washed with 2 N HCl (1 × 100 mL) and $NaHCO_3$ solutions (1 × 50 mL). The organic phase was dried over Na_2SO_4 and the solvent removed by reduced pressure. The residue was dissolved in chloroform (2–4 mL), precipitated in methanol (500 mL) at 0 °C and the black solid, with metallic shine, was further extracted with ethanol and *n*-hexane.

*2.4.1.1. Copolymer **P1**.* Compound **M1** (82 mg, 0.25 mmol), **M2** (103 mg, 0.25 mmol), $Pd(PPh_3)_4$, (9 mg), THF (4 mL). The black solid was dried under vacuum for 1 day to give the final product **P1** (46 mg, 25%). UV: λ_{max} (lg ε [L × mol^{-1} × cm^{-1}]) 468 nm (5.90), Eg_{sol} = 2.21 eV. Emission: λ_{max}: 567 nm. UV: $\lambda_{max,film}$ 551 nm, Eg_{film} = 1.85 eV. FT-IR spectra (cm^{-1}): 2926 (s, CH_3, stretching), 2851 (s, CH_2, stretching), 1448 (m, C=C, stretching), 1373 (s, =CH, stretching), 1167 (m, C–N, stretching), 781 (s, =C–H, out-of-plane deformation). GPC (g/mol): M_n = 8200, M_w = 14900, PDI: 1.82. ^{1}H NMR (400 MHz, $CDCl_3$): δ (ppm): 7.01 (s, 3H), 2.77 (s, 2H), 1.68 (s, 2H), 1.25 (d, 6H), 0.88 (s, 3H). Anal. Calcd. For **P1**; C, 67.15; S, 25.61; H, 7.24; Found C, 67.45; S, 25.26; H, 7.29%.

*2.4.1.2. Copolymer **P2**.* Compound **M3** (157 mg, 0.25 mmol), **M2** (103 mg, 0.25 mmol), $Pd(PPh_3)_4$, (9 mg), THF (4 mL). The black solid was dried under vacuum for 1 day to give the final product **P2** (57 mg, 22%). UV: λ_{max} (lg ε [L × mol^{-1} × cm^{-1}]) 493 nm (5.74), 384 nm (3.90), Eg_{sol} = 2.13 eV. Emission: λ_{max}: 662 nm. UV: $\lambda_{max,film}$ 542/401 nm, Eg_{film} = 1.81 eV. FT-IR spectra (cm^{-1}): 2926 (s, CH_3, stretching), 2851 (s, CH_2, stretching), 1448 (m, C=C, stretching), 1373 (s, =CH, stretching), 1167 (m, C–N, stretching), 781 (s, =C–H, out-of-plane deformation). GPC (g/mol): M_n = 7900, M_w = 16000, PDI: 2.03. ^{1}H NMR (400 MHz, $CDCl_3$): δ (ppm): 7.69 (s, 2H), 7.22 (s, 2H), 7.11 (s, 2H), 2.77 (s, 4H), 1.68 (s, 4H), 1.25 (d, 12H), 0.86 (s, 4H). Anal. Calcd. For **P2**; C, 65.41; S, 23.28; H, 6.22; N, 5.09; Found C, 65.56; S, 22.8; H, 6.58; N, 5.06%.

2.4.2. Copolymers *P3* and *P4*—general procedure

4,7-*Bis*-(5-bromo-3-hexyl-thiophen-2-yl)-benzo[*c*][1,2,5]-thiadiazole, 2,5-*bis*-(trimethylstannyl)-thiophene and $Pd(PPh_3)_4$ (5 mol %) were added together in a microwave tube. Under argon, THF (4 mL) was added to the reaction system and was allowed to stir in the microwave for 12 min at 150 °C. Subsequently, the reaction system was endcapped by using 4-bromobenzenethiol for 2 min at 150 °C. After cooling down to room temperature the reaction solution was poured in chloroform and the combined organic layers were washed with 2 N HCl (1 × 100 mL) and $NaHCO_3$ solutions (1 × 50 mL). The organic phase was dried over Na_2SO_4 and the solvent removed by reduced pressure. The residue was dissolved in chloroform (2–4 mL), precipitated in methanol (500 mL) at 0 °C and the black solid, with metallic shine, was further extracted with ethanol and *n*-hexane.

*2.4.2.1. Copolymer **P3**.* Compound **M1** (82 mg, 0.25 mmol), **M2** (103 mg, 0.25 mmol), $Pd(PPh_3)_4$, (9 mg), THF (4 mL). The black solid was dried under vacuum for 1 day to give the final product **P3** (44 mg, 24%). UV: λ_{max} (lg ε [L × mol^{-1} × cm^{-1}]) 464 nm (5.88), Eg_{sol} = 2.20 eV. Emission: λ_{max}: 621 nm. UV: $\lambda_{max,film}$ 540 nm, Eg_{film} = 1.84 eV. FT-IR spectra (cm^{-1}): 3067 (w, Ar–H), 2926 (s, CH_3, stretching), 2851 (s, CH_2, stretching), 1448 (m, C=C, stretching), 1373 (s, =CH, stretching), 1167 (m, C–N, stretching), 781 (s, =C–H, out-of-plane deformation). GPC (g/mol): M_n = 8000, M_w = 15000, PDI: 1.88. ^{1}H NMR (400 MHz, $CDCl_3$): δ (ppm): 7.01 (s, 3H), 2.77 (s, 2H), 1.68 (s, 2H), 1.25 (d, 6H), 0.88 (s, 3H). Anal. Calcd. For **P3**; C, 67.15; S, 25.61; H, 7.24; Found C, 66.82; S, 25.97; H, 7.21%.

*2.4.2.2. Copolymer **P4**.* Compound **M3** (157 mg, 0.25 mmol), **M2** (103 mg, 0.25 mmol), $Pd(PPh_3)_4$, (9 mg), THF (4 mL). The black solid was dried under vacuum for 1 day to give the final product **P4** (52 mg, 20%). UV: λ_{max} (lg ε [L × mol^{-1} × cm^{-1}]) 489 nm (5.60), 382 nm (4.14), Eg_{sol} = 2.13 eV. Emission: λ_{max}: 683 nm. UV: $\lambda_{max,film}$ 540/396 nm, Eg_{film} = 1.80 eV. FT-IR spectra (cm^{-1}): 3067 (w, Ar–H), 2926 (s, CH_3, stretching), 2851 (s, CH_2, stretching), 1448 (m, C=C, stretching), 1373 (s, =CH, stretching), 1167 (m, C–N, stretching), 781 (s, =C–H, out-of-plane deformation). GPC (g/mol): M_n = 7700, M_w = 15500, PDI: 2.01. ^{1}H NMR (400 MHz, $CDCl_3$): δ (ppm): 7.69 (s, 2H), 7.22 (s, 2H), 7.11 (s, 2H), 2.77 (s, 4H), 1.68 (s, 4H), 1.25 (d, 12H), 0.86 (s, 4H). Anal. Calcd. For **P4**; C, 65.41; S, 23.28; H, 6.22; N, 5.09; Found C, 65.67; S, 22.59; H, 6.67; N, 5.07%.

2.5. Synthesis of the PbS NPs—general procedure

The PbS nanoparticles were synthesized using tri-*n*-octylphosphine and oleic acid as stabilizing agents [45,46]. As synthetic equipment a three-neck flask with condenser, a thermocouple, heating mantle and magnetic stirrer were used. Typically, a mixture of 0.78 g lead acetate trihydrate (2 mmol), 1.5 mL oleic acid (4.7 mmol), 4 mL distilled tri-*n*-octylphosphine (9 mmol) and 6 mL diphenylether (38 mmol) were heated under vacuum for 1 h at 80 °C. The sulfur precursor solution, comprising 0.05 g thioacetamide (0.67 mmol), 0.25 mL *N*,*N*-dimethylformamide (3.3 mmol) and 6 mL tri-*n*-octylphosphine (13.5 mmol) was injected at 150 °C under nitrogen and the reaction was quenched after 5 min. Subsequently, the particle solution was cleaned by precipitation from 1-butanol. The precipitate was washed two times with 1-butanol and afterwards re-dissolved in an organic solvent. For spectroscopic investigations tetrachloroethylene or toluene were used as solvents.

2.6. Synthesis of the PbS-copolymer composites—general procedure

In general, PbS-copolymer composites **NC3** and **NC4** were synthesized by treatment of PbS nanoparticles with **P3** and **P4**. First, the PbS nanoparticles (5 mg) were mixed in 1 mL of a solution of THF with the thiol-functionalized polymer (10 mg/mL) and stirred overnight. After precipitation from ethanol, washing two times with *n*-butanol and drying under vacuum, two nanocomposite (NC)-like materials **NC3** and **NC4** were obtained as powders.

2.7. Fabrication and measurement of the solar cells

Solar cells were fabricated on ITO-coated glass substrates (ShinAn SNP, $R_{□}$ = 13 Ω/□), which were cleaned in acetone and *iso*propanol by ultrasonication for 15 min each. Subsequently, the substrates were exposed to oxygen plasma and transferred into a glove box, where they were kept under nitrogen atmosphere for the rest of the fabrication and characterization process. A layer of low-conductive PEDOT:PSS (Clevios™ P VP AI 4083) was spin-casted onto the substrate followed by the active layer from a blend comprising the polymers **P3**, **P4** or the nanocompound **NC3**

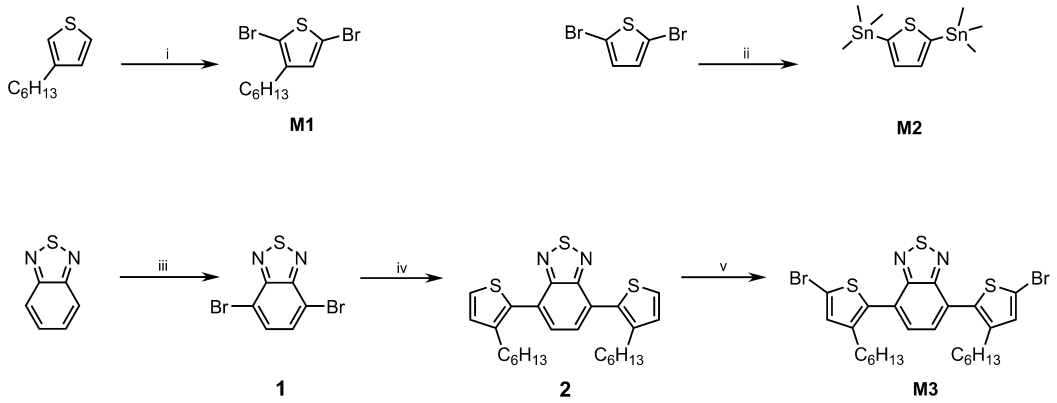

Scheme 1. Synthesis of **1**, **2** and monomers **M1**–**M3**. Reagents and conditions: (i) NBS, THF, 0 °C, 4–5 h; then rt, overnight; (ii) THF, *n*-BuLi, −78 °C, 4–5 h, then trimethyltin chloride 1 M in *n*-hexane, −78 °C, then rt, overnight; (iii) Br_2, HBr(aq), reflux, overnight; (iv) 2-(3-hexylthiophen-2-yl)-4,4,5,5-tetramethyl-1,3,2-dioxaborolane, $Pd(PPh_3)_4$, toluene, EtOH, H_2O, Na_2CO_3, reflux, overnight; (v) NBS, THF, 0 °C, 4–5 h; then rt, overnight.

and $PC_{60}BM$ at concentrations of 30 mg/mL from 1,2-dichlorobenzene. The active layer thickness was on the order of 70 nm. The cells were completed by the evaporation of calcium cathodes through a shadow mask in high vacuum. Current density/voltage (J-V) curves were recorded utilizing a Keithley 238 source meter unit under 1 sun illumination according to the AM 1.5G spectrum utilizing a spectrally monitored Oriel 300W solar simulator. For the IPCE measurement, the solar cells were encapsulated in order to avoid sample degradation. The IPCE setup features a 450 W Xenon light source, a 300 mm monochromator (LOT-Oriel GmbH & Co KG), a custom designed current amplifier (DLPCA-S Femto Messtechnik GmbH) and a digital lock-in (eLockinin203 Anfatec). A modified photoreceiver (OE-200-S Femto Messtechnik GmbH) with a Si/InGaAs sandwich diode was used to monitor the stability of the monochromatic light beam. Initial calibration in the infrared spectral regime was carried out with a reference germanium diode (NIST traceable calibration, Thorlabs).

3. Results and discussion

2,5-Dibromo-3-hexyl-thiophene (**M1**, yield: 69%) was obtained through bromination of 3-hexyl-thiophene by using *N*-bromo-succinimide (NBS) [47]. 2,5-*Bis*-(trimethylstannyl)-thiophene (**M2**, yield: 46%) was synthesized in a two-step reaction by lithiation of thiophene at −78 °C, followed by stannylation of the intermediate with trimethyltin chloride (Scheme 1) [48]. For the synthesis of 4,7-*bis*-(5-bromo-3-hexyl-thiophen-2-yl)-benzo[*c*][1,2,5]-thiadiazole (**M3**, yield: 65%), 2,1,3-benzothiadiazole was used as starting material, firstly brominated to give compound **1** (yield: 90%) and then coupled to 2-(3-hexylthiophen-2-yl)-4,4,5,5-tetramethyl-1,3,2-dioxaborolane following a Suzuki-protocol [10,11,44,49–51] yielding compound **2** in 70% (Scheme 1). Compound **2** was ongoing transformed to the final product **M3** by bromination with NBS (Scheme 1) [52–54]. Alternating copolymers based on **M1**-**M3** were synthesized by microwave-assisted Stille-coupling reactions according to optimized Pd(0)-mediated Stille-C-C-coupling protocols (Scheme 2) [44,55]. Using **M1** or **M3** in combination with comonomer **M2**, the thiophene-based alternating copolymers **P1** and **P2** were obtained.

Copolymers **P1** and **P2** were further treated with 4-bromobenzenethiol in order to terminate their backbones at the stannylated reaction site, ending up with polymers **P3** and **P4**, respectively (Scheme 2). The yields of the crude copolymers **P1**–**P4** are in the range of 30–35% based on the sum of molecular weights of the comonomers.

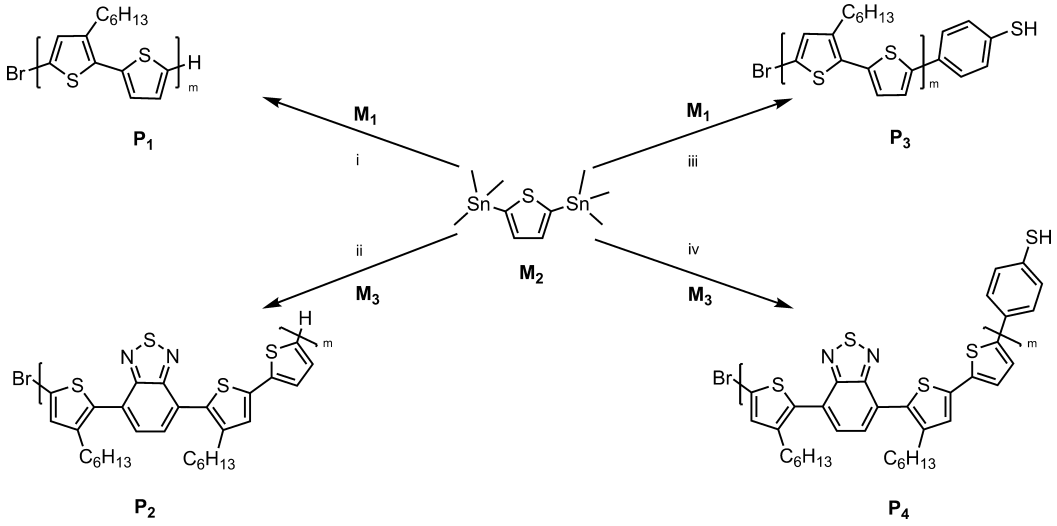

Scheme 2. Synthesis of polymers **P1**–**P4**. Reagents and polymerization parameters under microwave assisted conditions: (i) **M1**, **M2**, $Pd(PPh_3)_4$, THF, 150 °C, 12 min; (ii) **M2**, **M3**, $Pd(PPh_3)_4$, THF, 150 °C, 12 min; (iii) **M1**, **M2**, $Pd(PPh_3)_4$, THF, 150 °C, 12 min, then 4-bromobenzenethiol, 150 °C, 2 min; (iv) **M2**, **M3**, $Pd(PPh_3)_4$, THF, 150 °C, 12 min, then 4-bromobenzenethiol, 150 °C, 2 min.

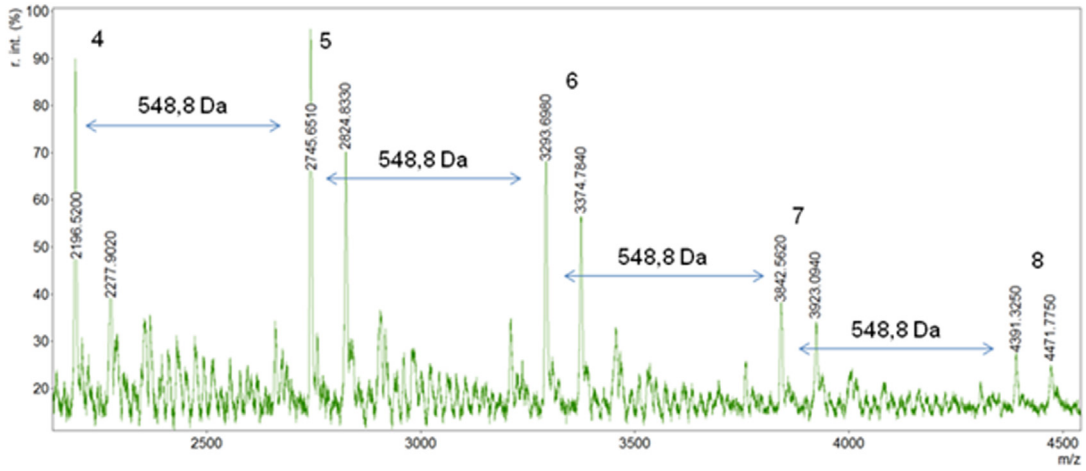

Fig. 1. MALDI-TOF mass spectrum of **P2**.

However, in order to remove impurities and low molecular weight species, and to thus obtain unimodal molecular weight distributions, the crude polymers **P1**–**P4** were exhaustively purified by extractions with methanol, *n*-hexane and chloroform. Each step was carried out over a period of 1 day by means of a Soxhlet-apparatus, whereby the chloroform fraction was isolated and re-precipitated from methanol. After purification, the copolymers were obtained as dark black solids with a metallic shine still in yields of 20–25%, readily soluble in solvents of medium polarity like tetrahydrofuran (THF) or dichloromethane. Highly soluble copolymers are of importance allowing facile solution processing [56–63], which has to be ensured especially when modern device design is envisaged. Due to their thiol-functionality, copolymers **P3** and **P4** may be suitable for tying on inorganic nanoparticles giving the opportunity to create hybrid materials *via* a ligand exchange procedure [1,11,64] on the surface of the nanoparticles, in this case, lead sulfide nanoparticles (PbS). The structures of the monomers and copolymers were confirmed by using ^{1}H and ^{13}C NMR and their molecular weights were determined by means of electrospray ionization mass spectrometry (ESI-MS) and gel permeation chromatography (GPC) analysis, correspondingly. The structures of the copolymers **P1**–**P4** were additionally confirmed by elemental analysis. The molecular weights of the polymers **P1**–**P4** were determined by GPC using chloroform as eluent and a calibration based on polystyrene standards [65]. However, thiophene-based polymers adopt a more rod-like conformation in solution and because of this GPC measurements performed on the basis of polystyrene standards tend to overestimate the molecular weights in such systems [65]. Nonetheless, as determined by GPC, these four polymers have similar weight-average molecular weights (M_w) of around 14900–16000 g $\times$ mol^{-1}, corresponding to a polydisperity index (PDI) in-between 1.82–2.03. On the other hand, the discussed GPC-determined values are in close agreement with values in present literature using similar synthetic methods and GPC standards [66,67]. In order to further determine the uniformity of the polymers, MALDI-TOF analysis was conducted [67–69]. Contradictive to GPC MALDI-TOFMS tends to underestimate the molecular weights of polydisperse polymers, because efficient desorption is hindered at higher molecular weights of the polymers [70,71]. Nonetheless, effective ionization and desorption are necessary in order to obtain MALDI-TOF spectra of high quality. Note the choice of the matrix and the optimized sample preparation for each individual type of polymer is significant [72]. However, by using MALDI-TOF analysis an accurate picture of the distribution of chains with respect to the obtained end groups is possible. Since in the Stille cross-coupling procedure the respective copolymer may end with either of the two applied monomers (A and B), different distributions of the end groups are expected. Hummelen et al. [67] found that all of the polymer chains, which are prepared by the Stille method show three distinct peaks corresponding to X^BX_n, X_n and X_nX^A–through copolymerization of two monomers X^A and X^B are the molecular weight peaks of the two monomers A and B and X_n is equivalent to $(X^AX^B)_n$ [67].

The analysis of the MALDI-TOF mass spectrum of i.e. **P2** (Fig. 1) shows a distribution of the most probable peak at 2745.6 Da. Each

Table 1
Optical properties of copolymers **P1**–**P4**.

Polymer	Abs_{sol}[a] (nm) Lg ε ([L $\times$ mol^{-1} $\times$ cm^{-1}])	Abs_{film} (nm)	Eg_{sol}[a,b] (eV)	Eg_{film}[b,c] (eV)
P1	468 (5.90)	551	2.21	1.85
P2	493 (5.74)/384 (3.90)	542/401	2.13	1.81
P3	464 (5.88)	540	2.20	1.84
P4	489 (5.60)/382 (4.14)	540/396	2.13	1.80

[a] In chloroform solution (3.3 $\times$ 10^{-6} mol/L).
[b] Calculated from the absorption band edge.
[c] Determined on glass.

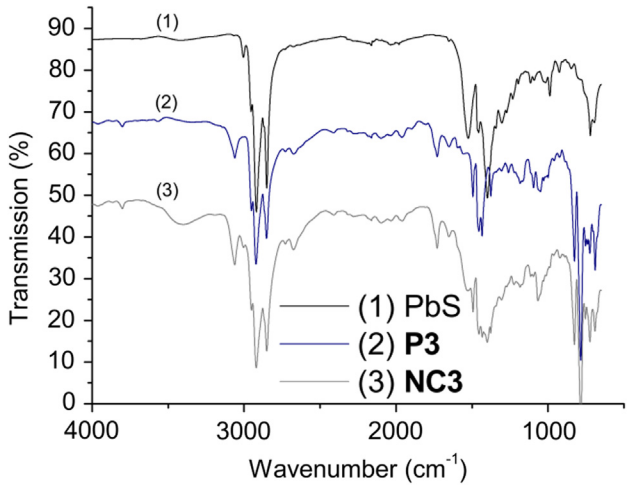

Fig. 2. FT-IR-spectra of PbS, **P3**, and nanocomposite **NC3**.

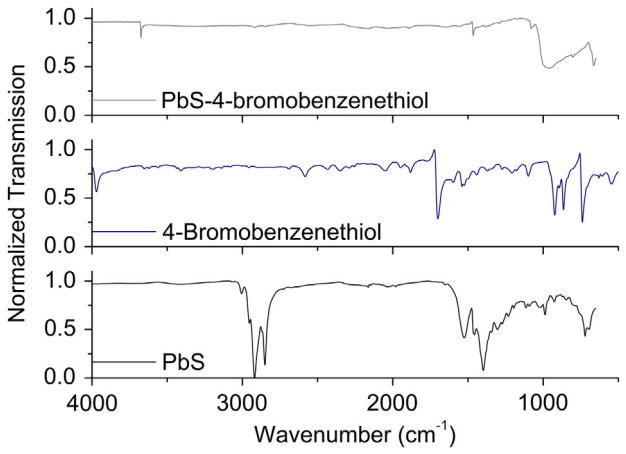

Fig. 3. FT-IR-spectra of PbS, 4-bromobenzenethiol and PbS-(4-bromobenzenethiol).

peak in this spectrum is representative of a different degree of polymerization. The peak-to-peak distance amounts to 548.8 Da and reflects the mass of the two monomer repeating units. There are two absolute masses of each of the signals of the polymer distribution (i.e. 2745.7 and 2824.8 Da), from which the end groups can be calculated. This respective mass values are composed of the number n of repeating units with a molecular weight of 550 Da and the masses of two of the probable end groups. The number n is determined by the fraction i.e. 2745.7 Da/548.8 Da = 5.003. The masses of both end groups are then given by multiplying the residual value 0.003 by 548.8 Da = 1.7 Da. The mass of end groups of the other peak is 80.8 Da. From this, together with the knowledge of the starting and the terminating reaction of Stille copolymerized copolymers, the most probable end groups in our case are H/Br and H/H, respectively. Since the copolymers were, after the extensive Soxhlet-extraction, not further subjected to i.e. preparative GPC, in order to remove the small amount of homofunctional species, we note these homofunctional species were present during the ongoing study.

Due to their favorable solubility, all four copolymers can be readily cast into uniform thin films, rendering them good candidates for the fabrication of organic semiconductor devices [1–11,26,31,44,56–59,61–64]. Their optical properties are summarized in Table 1. A blue shift is observed when comparing the absorption maxima of copolymers **1** and **3** in solution and solid state. Such a shift is also pronounced in case of copolymers **P2** and **P4**. In solid-state, copolymers **P1**–**P4** revealed low bandgaps of 1.80–1.85 eV (Table 1). Changing the electron-rich thiophene moiety in copolymers **P1**, **P3** with the electron-deficient benzothiadiazole moiety available in copolymers **P2** and **P4**, a lowering of the bandgap is targeted for the latter. Comparing the "donor–donor"-type copolymers **P1** and **P3** with the "donor-acceptor"-type **P2** and **P4**, a similarity in the bandgaps of all copolymers was observed. This result proposes that solely the addition of the benzothiadiazole moiety is not enough to greatly decrease the bandgap within these copolymers as the conjugation length influenced by the torsional strain along the backbone of the achieved macrocompounds is directly related to energy bandgap, whereby greater bond-length alternation can lead to larger E_g [73,74].

The PbS NPs were thus subjected to a ligand exchange by treatment with both thiol-functionalized copolymers **P3** and **P4**. Before the ligand exchange took place, the nanoparticles were stabilized with the ligands oleic acid and tri-*n*-octylphosphine. After precipitation with ethanol, washing with *n*-butanol and drying under vacuum, two nanocomposite (NC)-like materials **NC3** and **NC4** were obtained as powders. As exemplified in Fig. 2, Fourier-transform-infrared (FT-IR) measurements show that the PbS-copolymer **3** spectrum is an addition of the PbS and the respective copolymer **P3** spectrum, which also holds true when using **P4**. The thiol-functionality of the copolymer and the bonding of this functionality to the PbS-nanoparticles are not clearly displayed in the spectra due to the dominating copolymer bands. Therefore, one cannot evidently distinguish whether the copolymer is bound to the nanoparticle surface without a doubt, or if it is only a mixture of both counterparts.

To unmistakably prove the ligand exchange, the sole thiol-functional endcapper molecule 4-bromobenzenethiol was used. Fig. 3 shows that the CH_2- and CH_3-stretching vibrations (2750–3100 cm^{-1}) and the CH_2- and CH_3-bending vibrations (1300-1600 cm^{-1}) of the oleic acid do not exist any longer in the PbS-(4-bromobenzenethiol) FT-IR spectrum. This could also be the case for the nanocomposites **NC3** and **NC4**; the presence, however, of methylene-groups in the side-chains of the organic counterpart cover this disappearance (Fig. 2). The same vanishing phenomenon occurs for the SH-vibration, coming at 2564 cm^{-1} in the 4-bromobenzenethiol spectrum. This means that the thiol-functionalities of 4-bromobenzenethiol are now bound to the surface of the PbS NPs and the oleic acid was exchanged by the thiol-functionalized bromobenzene. Assuming the affinity of the thiol-group of the macroligands **P3** and **P4** is the same as the affinity

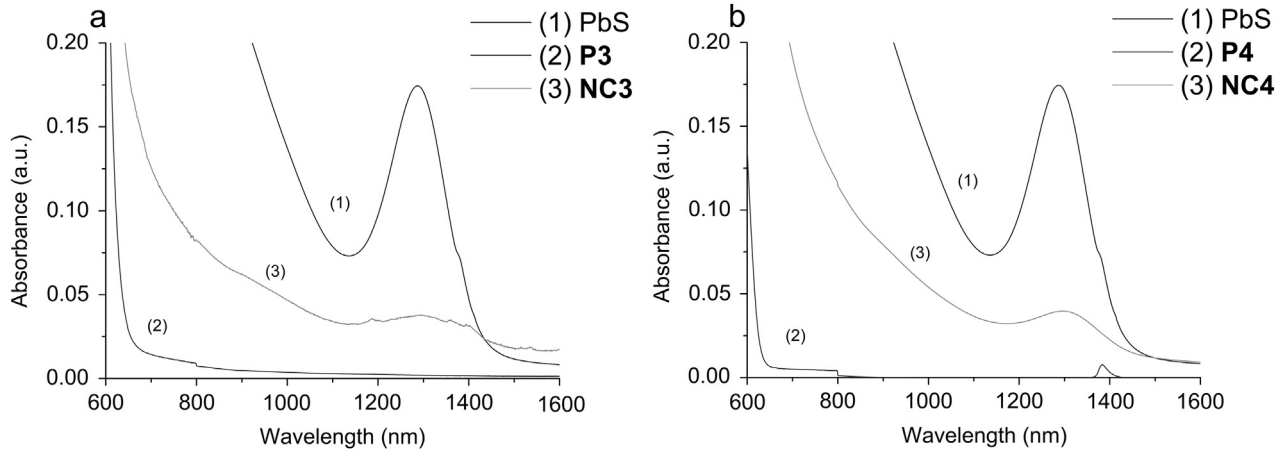

Fig. 4. Absorption spectra (in tetrachloroethylene) of copolymer **P3**, PbS and **NC3** (a) and copolymer **P4**, PbS and **NC4** (b).

Table 2
Absorption and emission maxima of copolymers **P3** and **P4** as well as of composites **NC3** and **NC4**.

Material	Abs UV-vis (nm)[a]	Abs near IR (nm)[b]	Em UV-vis (nm)[a]	Em near IR (nm)[b]
P3	496	–	683	–
P4	463	–	621	–
NC3	498	1294	673	1333
NC4	476	1297	624	1339

Solutions in toluene[a] or tetrachloroethylene[b] (5 mg **NC3/4**/mL). Abs max PbS[b]: 1286 nm; Em max PbS[b]: 1326 nm.

of the small-molecular endcapper, the covalent interconnection between the thiol-functionality of the copolymers **P3** and **P4** and the PbS nanoparticles is very likely.

The optical properties of the **NCs** were investigated and compared to that of the copolymers **P3** and **P4** and the bare PbS nanoparticles (Fig. 4). Note, like the analysis of the copolymers, the analysis of the composites has also been carried out at similar concentrations. Investigating the optical properties in the near infrared region, a change in the intensity of the respective composite spectrum is observed, revealing characteristics of the individual PbS and copolymer spectra, which seem to interact with each other and establish optical properties of the supposed composite material (Fig. 4). In more detail, the PbS particles analyzed in tetrachloroethylene revealed an absorption maximum at 1286 nm. Connecting **P3** to these PbS particles, a slight red-shift to 1294 nm was observed in the near-infrared and in case of binding **P4** to the PbS surfaces, the maximum was shifted to 1297 nm (Table 2). The absorption bands of **NC3** (Fig. 4a) and **NC4** (Fig. 4b), analyzed in tetrachloroethylene, are extended to near-infrared wavelengths, when compared to the absorption bands of the neat copolymers **P3** and **P4**. The UV-vis spectral analysis (Fig. 5a) in toluene was moreover carried out providing absorption maxima for **P3** at 496 nm and 463 nm for **P4**, respectively. After connecting the PbS particles to the polymer macroligands, **NC3** revealed an absorption maximum at 498 nm and **NC4** at 476 nm, correspondingly. Thus, in case of transforming **P4** to **NC4**, a red-shift of 13 nm was observed (Table 2). This is further evidence in terms of deciphering the constitutional features of **NC3** and **NC4**, corroborating the assumption for the successful copolymer-nanoparticle interconnection. Though the predomination of a nanoparticle-like absorption (Fig. 4), which is correlated to the higher electron affinity of nanoparticles compared to conjugated polymers [75], such combinative spectrum patterns are not unusual for composite-like materials [11].

In addition to the absorption properties, the emission in toluene of **P3** and **P4** compared to **NC3** and **NC4** have been investigated, respectively (Fig. 5b). While in the near-infrared region, the emission maximum of the PbS particles was detected at 1326 nm, there are slight spectral changes to the red for the composite materials; namely for **NC3** the maximum was found at 1333 nm and for **NC4** the maximum was observed at 1339 nm (Table 2). Some further differences were observed in the UV-vis spectral region (Fig. 5b). Here, **P3** revealed an emission maximum at 683 nm and **P4** at 621 nm, correspondingly, while **NC3** emitted at 673 nm likewise **NC4** at 624 nm.

The uniform shape and size (about 3.8–4.8 nm) of the PbS NPs (Fig. 6a) was monitored by transmission electron microscopy (TEM). The PbS NPs reveal a low bandgap of 0.73 eV, which corresponds to a wavelength of about 1680 nm (onset derived from Fig. 4). Furthermore, these PbS NPs indicate an appropriately low bandgap, which principally suggests potential charge transfer in photodiode applications [9] when paired with suitable copolymers or macroligands. Moreover, the color changes observed when comparing bare PbS particles, copolymers and composites **NC3**–**4** (Fig. 6b and c) may be brought in connection with side- or end groups present in the macrocompounds influencing the surface states of the nanoparticles [76]. Further evidence for this is given by the TEM micrographs of **NC3** and **NC4** shown in Fig. 6d and e.

In order to examine the photovoltaic properties of the polymers synthesized before, bulk heterojunction solar cells comprising active layers from **P3** or **P4** blended with $PC_{60}BM$ at different blending ratios were fabricated. It was generally found that solar cells comprising **P3**:$PC_{60}BM$ blends produce higher photocurrents than **P4**:$PC_{60}BM$-based solar cells. Consequently, the corresponding nanocompound **NC3** was chosen for the investigation of the ternary hybrid photovoltaic devices. The incorporation of PbS (**NC3**) leads to a significant reduction of all photovoltaic key performance parameters: The PbS-free solar cell, exhibits an open circuit voltage V_{OC} of 608 mV, a short circuit current density j_{SC} of 2.5 mA/cm^2 and a fill factor FF of 33% resulting in an overall power conversion efficiency PCE of 0.5%. When replacing **P3** with nanocomposite **NC3** the key performance parameters are reduced to V_{OC} = 210 mV, j_{SC} = 0.34 mA/cm^2 and a FF = 24%, which results in a PCE = 0.02%. This performance decrease upon the incorporation of PbS *via* **NC3** can be attributed to the low bandgap of PbS; the nanoparticles can act as recombination centers for photo-generated excitons leading to a simultaneous decrease in V_{OC}, j_{SC}, FF and PCE. However a

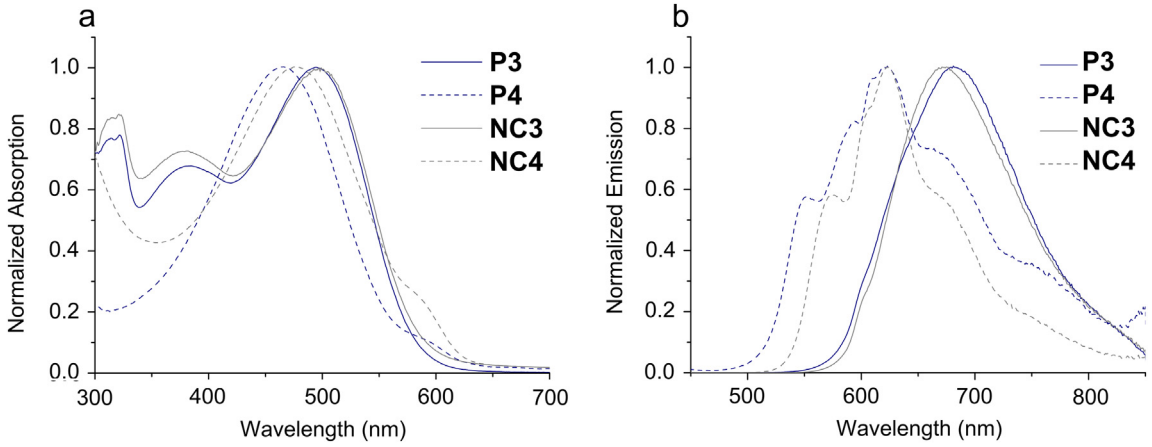

Fig. 5. Absorption (a) and emission (b) spectra (in toluene) of copolymer **P3** (blue, solid), **NC3** (gray, solid) **P4** (blue, dash), and **NC4** (gray, dash). (For interpretation of the references to color in this figure legend, the reader is referred to the web version of this article.)

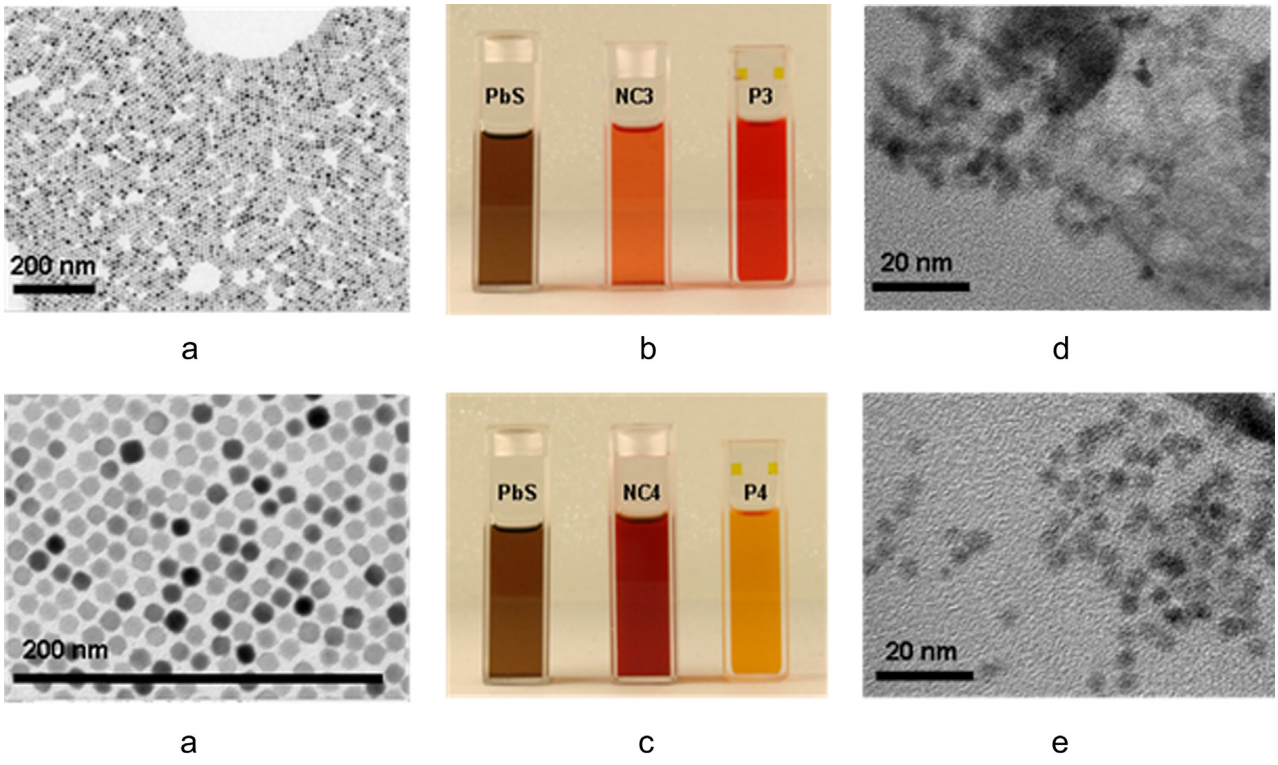

Fig. 6. TEM micrographs of PbS NPs (a), **NC3** (d) and **NC4** (e) and photographs (in tetrachlorethylene solutions) of PbS, **NC3**, copolymer **P3** (b) and PbS, **NC4**, copolymer **P4** (c).

contribution of PbS in **NC3** to the photo current becomes evident in incident photon to electron conversion efficiency (IPCE) measurements in the infrared part of the visible spectrum as depicted in Fig. 7a and b . While a peak becomes visible around 1200 nm in the IPCE of the ternary blend, no IPCE signal was visible for the **P3**:$PC_{60}BM$ solar cells in this wavelength region. The IPCE peak position at 1200 nm corresponds nicely to the PbS and **NC3** absorption in Fig. 4. Therefore and despite the undesirable diminishment of the IPCE in the visible region, it can be concluded that the PbS nanoparticles within the nanocompound **NC3** harvest sunlight in the infrared and hence contribute to the photocurrent generation in the solar cell. Research efforts on enhancing the device performance upon varying the macroligands composition will be addressed in the near future.

4. Conclusions

In conclusion, near-infrared absorbing PbS nanoparticles, surface-modified with thiol-functional thiophene-based macroligands, have been synthesized in a well-designed procedure. FT-IR data confirm the formation of the surface bond between the macroligand's SH-groups and the PbS surface. The SH-functional copolymers have been developed using a convenient Stille-protocol optimized for C–C bond formation in the microwave. The thiol-function has been introduced using 4-bromobenzenethiol as end-functional moiety. The macroligand approach using thiol-functions offered a facile synthetic pathway to polymer-capped lead-based semiconductor NCs, where changing the macroligand design, the near-infrared absorption properties of the lead-based

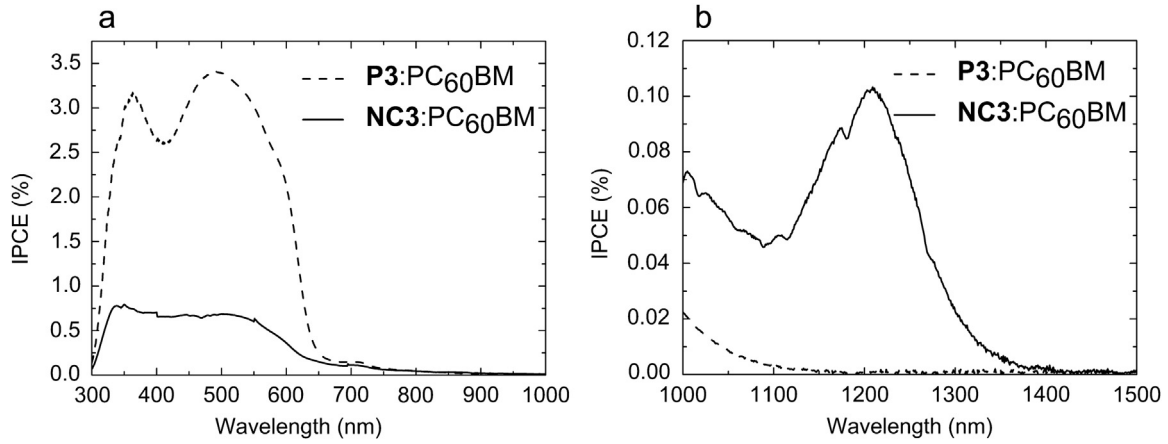

Fig. 7. IPCE Spectra of **P3**:$PC_{60}BM$ (1:1 wt.) and **NC3**:$PC_{60}BM$ (1:1 wt.) solar cells in 300 nm to 1000 nm (a) and 1000 nm to 1500 nm (b) wavelength regimes. The peak at 1200 nm for **NC3**:$PC_{60}BM$ devices can be attributed to a photocurrent generation on the PbS nanoparticles within the **NC3** compound.

NPs of the two organic-inorganic components can be individually manipulated (functional linker, backbone composition or NP size) offering well-defined organic and inorganic components that can reliably be interconnected to hybrid materials. The ability to solution-process these PbS-based hybrids is an important parameter for their future implementation in photovoltaic or optoelectronic applications. A second important key parameter of this approach is the fact that by changing the macroligand design, the electronic and optical properties, as well as the morphology of the differently capped PbS NPs can be influenced. The manipulation over the electronic and optical properties can play a crucial role towards the direction of improving hybrid devices.

Acknowledgments

E.H. acknowledges the Deutsche Forschungsgemeinschaft (DFG) for financial support within the collaborative projects HO3911/2-1 and RO2345/5-1: “Hybrid polymer/nanocrystals structures: fabrication and studies of energy transfer, charge generation and transport” both in collaboration with DFG SPP 1355 project HO3911/4-1: “Low bandgap dendrimer systems: Synthesis, spectroscopy and microscopy of composite films for photovoltaics”. E.H. acknowledges Prof. Ullrich Scherf for granting access to the tools of the Macromolecular Chemistry at the University of Wuppertal (BUW). S.G.H. gratefully acknowledges the EU network of excellence Nanophotonics4Energy. Dr. Karin Sahre of the Leibnitz-Institute of Polymer Research Dresden e.V. is acknowledged for performing the MALDI-TOFMS measurements.

References

[1] Liu J, Tanaka T, Sivula K, Alivisatos AP, Frechet JMJ. J Am Chem Soc 2004;126:6550–1.
[2] Saunders BR, Turner ML. Adv Colloid Interface Sci 2008;138:1–23.
[3] Palaniappan K, Murphy JW, Khanam N, Horvath J, Alshareef H, Quevedo-Lopez M, et al. Macromolecules 2009;42:3845–8.
[4] Skompska M. Synth Met 2010;160:1–15.
[5] Aldakov D, Jiu T, Zagorska M, de Bettignies R, Jouneau P-H, Pron A, et al. Phys Chem Chem Phys 2010;12:7497–505.
[6] Zhao L, Pang X, Adhikary R, Petrich JW, Lin Z. Angew Chem Int Ed 2011;50:3958–62.
[7] Zhao L, Pang X, Adhikary R, Petrich JW, Jeffries-El M, Lin Z. Adv Mater 2011;23:2844–9.
[8] Reiss P, Couderc E, Girolamo JD, Pron A. Nanoscale 2011;3:446–89.
[9] Holder E, Tessler N, Rogach A. J Mater Chem 2008;18:1064–78.
[10] Kanelidis I, Ren Y, Lesnyak V, Gasse JC, Frahm R, Eychmüller A, et al. J Polym Sci Part A: Polym Chem 2011;49:392–402.
[11] Kanelidis I, Altintas O, Gasse JC, Frahm R, Eychmüller A, Holder E. Polym Chem 2011;2:2597–608.
[12] Seo J, Kim SJ, Kim WJ, Singh R, Samoc M, Cartwright AN, et al. Nanotech 2009;20:095202/1–095202/6.
[13] Koleilat GI, Levina L, Shukla H, Myrskog SH, Hinds S, Pattantyus-Abraham AG, et al. ACS Nano 2008;2:833–40.
[14] Hoyos M, Turner ML, Navarro O. Curr Org Chem 2011;15:3263–90.
[15] Loewe RS, Ewbank PC, Liu J, Zhai L, McCullough RD. Macromolecules 2001;34:4324–33.
[16] Milliron DJ, Alivisatos AP, Pitois C, Edder C, Fréchet JMJ. Adv Mater 2003;15:58–61.
[17] Locklin J, Patton D, Deng S, Baba A, Millan M, Advincula R. Chem Mater 2004;16:5187–93.
[18] Noone KM, Strein E, Anderson NC, Wu PT, Jenekhe SA, Ginger DS. Nano Lett 2010;10:2635–9.
[19] Forrest SR. Nature 2004;428:911–8.
[20] Efros AlL, Efros AL. Sov Phys Semicond 1982;16:772–5.
[21] Mukherjee M, Datta A, Pradhan SK, Chakravorty D. J Mater Sci Lett 1996;15:654–7.
[22] Nagel M, Hickey SG, Froemsdorf A, Kornowski A, Weller H. Z Physikal Chem 2007;221:427–37.
[23] Lipovskii A, Kolobkova E, Petrikov V, Kang I, Olkhovets A, Krauss T, et al. Appl Phys Lett 1997;71:3406–8.
[24] Brumer M, Kigel A, Amirav L, Sashchiuk A, Solomesch O, Tessler N, et al. Adv Funct Mater 2005;15:1111–6.
[25] Rogach AL, Eychmüller A, Hickey SG, Kershaw SV. Small 2007;3:536–57.
[26] Kershaw SV, Susha AS, Rogach AL. Chem Soc Rev 2013;42:3033–87.
[27] Kanelidis I, Vaneski A, Lenkeit D, Pelz S, Elsner V, Stewart RM, et al. J Mater Chem 2011;21:2656–62.
[28] Adachi S. Properties of group-IV, III-V and II-VI semiconductors. John Wiley & Sons; 2005, ISBN 0-470-09032-4; 2005. p. 234.
[29] Guerreiro T, Ten S, Borrelli NF, Butty J, Jabbour GE, Peyghambarian N. Appl Phys Lett 1997;71:1595–7.
[30] Lipovskii AA, Kolobkova EV, Olkhovets A, Petrikov VD, Wise F. Phys E 1999;5:157–60.
[31] Dutta AK, Ho TT, Zhang LQ, Stroeve P. Chem Mater 2000;12:1042–8.
[32] Lu C, Guan C, Liu Y, Cheng Y, Yang B. Chem Mater 2005;17:2448–54.
[33] Lim P, Low HY, Chin WS. J Phys Chem B 2004;108:13093–9.
[34] Leontidis E, Orphanou M, Kyprianidou-Leodidou T, Krumeich F, Caseri W. Nano Lett 2003;3:569–72.
[35] Bakueva L, Gorelikov I, Musikhin S, Zhao XS, Sargent EH, Kumacheva E. Adv Mater 2004;16:926–9.
[36] Zhao XS, Gorelikov I, Musikhin S, Cauchi S, Sukhovatkin V, Sargent EH, et al. Langmuir 2005;21:1086–90.
[37] Huang NM, Shahidan R, Khiew PS, Peter L, Kan CS. Colloids Surf A: Physicochem Eng Asp 2004;247:55–60.
[38] Hines MA, Scholes G. Adv Mater 2003;15:1844–9.
[39] Zhu JJ, Liu SW, Palchik O, Koltypin Y, Gedanken A. J Solid State Chem 2000;153:342–8.
[40] Zhou SM, Zhang XH, Meng XM, Fan X, Lee ST, Wu SK. J Solid State Chem 2005;178:399–403.
[41] Hens Z, Vanmaekelbergh D, Stoffels EJAJ, van Kempen H. Phys Rev Lett 2002;88:236803-1–236803-4.
[42] Yang YJ, He LY, Zhang QF. Electrochem Commun 2005;7:361–4.
[43] Barkhouse DAR, Pattantyus-Abraham AG, Levina L, Sargent EH. ACS Nano 2008;2:2356–62.
[44] Tsami A, Yang XH, Farrell T, Neher D, Holder E. J Polym Sci Part A: Polym Chem 2008;46:7794–808.
[45] Nagel M, Hickey SG, Frömsdorf A, Kornowski A, Weller H. J Phys Chem 2007;221:427–37.
[46] Warner JH, Watt AAR. Mater Lett 2006;60:2375–8.
[47] Chaloner PA, Gunatunga SR, Hitchcock PB. J Chem Soc Perkin Trans 1997;2:1597–604.
[48] van Pham C, Macomber RS, Mark Jr HB, Zimmer H. J Org Chem 1984;49:5250–3.
[49] Tian N, Aulin YV, Lenkeit D, Pelz S, Mikhnenko OV, Blom PWM, et al. Dalton Trans 2010;39:8613–5.
[50] Tian N, Lenkeit D, Pelz S, Fischer LH, Escudero D, Schiewek R, et al. Eur J Inorg Chem 2010;30:4875–85.
[51] Vancoillie G, Pelz S, Holder E, Hoogenboom R. Polym Chem 2012;3:1726–9.
[52] Mancilha FS, Dasilveira Neto BA, Lopes AS, Moriva Jr PF, Quina FH, Gonçalves RS, et al. Eur J Org Chem 2006:4924–33.
[53] Kim JJ, Choi HB, Lee JW, Kang MS, Song KH, Kang SO, et al. J Mater Chem 2008;18:5223–9.
[54] Hou JH, Chen HY, Zhang SQ, Yang Y. J Phys Chem 2009;113:21202–7.
[55] Tian N, Thiessen A, Schiewek R, Schmitz OJ, Hertel D, Meerholz K, et al. J Org Chem 2009;74:2718–25.
[56] Tekin E, Wijlaars H, Holder E, Egbe DAM, Schubert US. J Mater Chem 2006;16:4294–8.
[57] Tekin E, Holder E, Kozodaev D, Schubert US. Adv Funct Mater 2007;17:277–84.
[58] Marin V, Holder E, Wienk MM, Tekin E, Kozodaev D, Schubert US. Macromol Rapid Commun 2005;26:319–24.
[59] Holder E, Meier MAR, Marin V, Schubert US. J Polym Sci Part A: Polym Chem 2003;41:3954–64.
[60] Holder E, Schoetz G, Schurig V, Lindner E. Tetrahedron: Asymm 2001;12:2289–93.
[61] Marin V, Holder E, Schubert US. J Polym Sci Part A: Polym Chem 2004;42:374–85.
[62] Marin V, Holder E, Meier MAR, Hoogenboom R, Schubert US. Macromol Rapid Commun 2004;25:793–8.
[63] Marin V, Holder E, Hoogenboom R, Tekin E, Schubert US. Dalton Trans 2006;13:1636–44.
[64] Kanelidis I, Elsner V, Bötzer M, Butz M, Lesnyak V, Eychmüller A, et al. Polymer 2010;51:5669–73.
[65] Liu JS, Loewe RS, McCullough RD. Macromolecules 1999;32:5777–85.
[66] Liu J, McCullough RD. Macromolecules 2002;35:9882–9.
[67] Brouwer F, Alma J, Valkenier H, Voortman TP, Hillebrand J, Chiechi RC, et al. J Mater Chem 2011;21:1582–92.
[68] Langeveld-Voss BMW, Janssen RAJ, Spiering AJH, van Dongen JLJ, Vonk EC, Claessens HA. Chem Commun 2000:81–2.
[69] Enders C, Tanner S, Binder WH. Macromolecules 2010;43:8436–46.
[70] Loewe RS, McCullough RD. Chem Mater 2000;12:3214–21.
[71] Babudri F, Colangiuli D, Farinola G, Naso F. Eur J Org Chem 2002:2785–91.
[72] Kazuo O. R&D Rev Toyota CRDL 2006;41:29–34.
[73] Zhang Y, Zou J, Yip HL, Chen KS, Zeigler DF, Sun Y, et al. Chem Mater 2011;23:2289–91.
[74] Brédas JL. J Chem Phys 1985;82:3808–11.
[75] Guo F, Xie P. Chin J Chem 2009;27:1427–33.
[76] Agrawal M, Rubio-Retama J, Zafeiropoulos NE, Gaponik N, Gupta S, Cimrova V, et al. Langmuir 2008;24:9820–4.